eMBNMS 2003

In: Explosive Subaqueous Volcanism, J.D.L. White, J.L. Smellie, D.A. Clague (eds.), Geophysical Monograph 140, American Geophysical Union, 129-142.

Hyaloclastite From Miocene Seamounts Offshore Central California: Compositions, Eruption Styles, and Depositional Processes

Alicé S. Davis and David A. Clague

Monterey Bay Aquarium Research Institute, California, USA

Hyaloclastite deposits are abundant on mid-Miocene volcanic seamounts offshore central California. The glass compositions are predominantly evolved hawaiite and mugearite, although minor amounts of tholeiitic to alkalic basalt are also present. Textural features give evidence for different eruption styles. For the evolved, alkalic compositions, fragmentation occurred primarily in response to exsolution of magmatic gases as the magma approached and erupted on the seafloor. Textural features of pyroclasts suggest formation of lava fountains of limited size and height, depending on water depth. Monomict, clast-supported hyaloclastite of highly vesicular pyroclasts suggest limited dispersal and deposition near vent sites. Matrix-supported, polymict breccias are reworked and displaced by currents into deeper water. The narrow range of glass compositions extending over multiple layers of volcanic sandstone suggests deposition from a slurry of tephra and water directly related to an eruption. Basaltic hyaloclastite of vesicle-free, angular glass fragments from the deepest site apparently formed from quench granulation. Sulfur contents suggest eruption depths ranging from near sea level to over 2000 m for samples collected from 1300 to over 3400 m depth, implying large amounts of subsidence for these seamounts.

INTRODUCTION

Volcaniclastic deposits consisting largely of basaltic glass fragments have been described from a variety of tectonic settings. Despite a considerable variety of compositions, textural characteristics, and size of particles, all of these rocks may be loosely referred to as hyaloclastite if the main component is glass [*Fisher and Schmincke*, 1984]. Hyaloclastite comprises a large proportion of the material erupted on ocean islands [e.g: *Staudigel and Schmincke,* 1984; *Clague et al.,* 1995; *Moore and Chadwick,* 1995], with the largest amount generated as the volcano grows to near sea level [e.g. *Staudigel and Schmincke,* 1984]. Similar, deep water erupted deposits occur at off-axis seamounts at fast- and slow spreading centers [e.g. *Batiza et al.,* 1984; *Batiza and White,* 2000; *Davis and Clague,* 2000]. They also form a significant component of the sediment record at island arc volcanoes [*Gill et al.,* 1990] and have been reported from nearly flat-lying oceanic flood basalts north of the Hawaiian Islands [*Clague et al.,* 1995, 2002]. No eruption of these deposits in the deep ocean has ever been observed and relatively little is known about them because they are not easily accessible.

This paper describes hyaloclastite samples recovered from Miocene volcanoes located at the continental margin offshore central California. We use the glass compositions and the textural characteristics to interpret the eruptive and depositional processes and compare these hyaloclastites to similar deposits from other locations.

Explosive Subaqueous Volcanism
Geophysical Monograph 140
Copyright 2003 by the American Geophysical Union
10.1029/140GM08

2. GEOLOGIC SETTING

Davidson, Guide, Pioneer, Gumdrop, and Rodriguez seamounts are five volcanic structures located at the continental margin offshore central to southern California (Figure 1), that are unlike intraplate, ocean island volcanoes or near-ridge seamounts [*Davis et al.*, 2002]. Variable in size (~10 to ~50 km in length), these five seamounts are morphologically complex, northeast-southwest trending ridges rather than conical structures with essentially circular bases as is typical for ocean island or near-ridge volcanoes. Unlike most oceanic volcanoes, they lack summit calderas or pit craters. Instead, they consist of a series of cones aligned along parallel ridges that are separated by sediment-filled troughs. This northeast-southwest trending fabric, observed for many seamounts offshore southern California and Baja [e.g. *Lonsdale,* 1991; *Davis et al.*, 1995], reflects the ridge-parallel structure of the underlying ocean crust [*Davis et al.*, 2002]. However, $^{40}Ar/^{39}Ar$ laser fusion ages indicate multiple episodes of volcanism, younger by at least

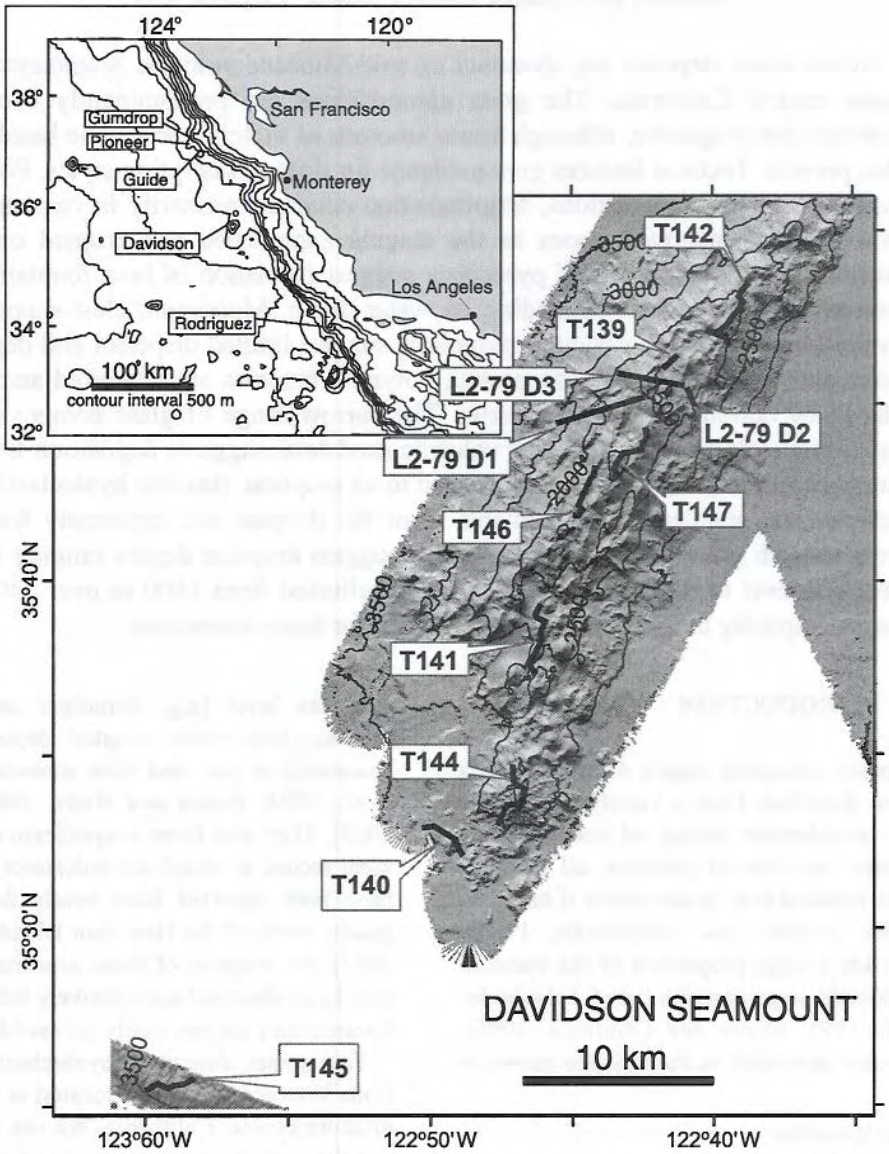

Figure 1A. Maps showing ROV tracks and dredge locations on (A) Davidson Seamount and (B) Guide Seamount. Inset map shows location of volcanic seamounts offshore central California.

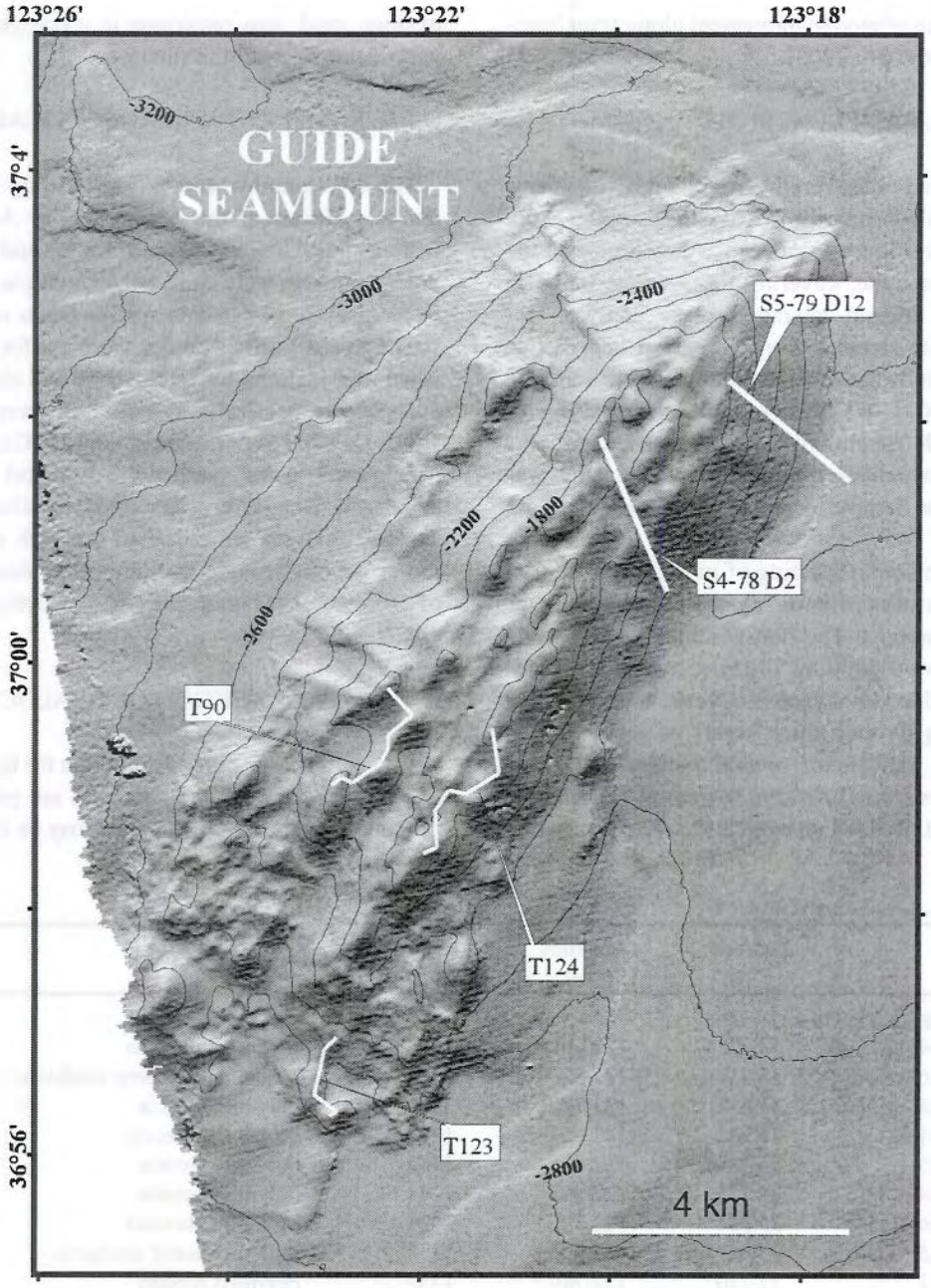

Figure 1B.

7 to 11 million years [*Davis et al.,* 2002] than the underlying ocean crust.

Volcanic rocks recovered from these seamounts are predominantly differentiated alkalic basalt, hawaiite, and mugearite. Isotopic compositions (Sr, Nd, Pb) indicate formation by small percentage of melting of variably enriched MORB-source-type mantle [*Davis et al.*, 2002]. The presence of mantle xenoliths in many samples suggests magma originated in the upper mantle. Xenoliths of alkalic cumulates and megacrysts of amphibole, feldspar, and titanomagnetite suggest extensive crystal fractionation occurred also in the upper mantle. Variable liquid lines of descent suggest small volumes of magma fractionally crystallized and erupted in isolated batches. Episodes of sporadic eruptions (16-10 Ma) presumably resulted from decompression melting of mantle rising along existing zones of weaknesses

undergoing extension related to movement along transform-fault systems [*Davis et al.,* 2002].

3. SAMPLING SITES

Hyaloclastite was recovered from each of these seamounts. We will primarily focus on samples from Davidson Seamount (Figure 1a), because they represent the most comprehensive suite, covering the greatest range in collection depths. Several averaged glass analyses for dredged hyaloclastite samples from Davidson and dredge and dive samples from the other seamounts were reported by *Davis et al.* [2002]. We include additional analyses of samples from Guide Seamount (Figure 1b), because the compositionally most diverse polymict hyaloclastite was recovered at that site. Sample locations and water depths are given in Table 1.

Hyaloclastite outcrops, consisting of more or less continuous flat, slabby surfaces (Figure 2a), are found at the tops of each of the seamounts. The non-vesicular hyaloclastite from the deepest dive (~3400 m, T145) occurred as discontinuous, crudely bedded, manganese-covered outcrops (~10 m high), protruding through thick layers of sediment. An outcrop of bedded sandstone, several meters high, was observed on one dive on Davidson Seamount (Figure 2b) but was not sampled. Bedded volcaniclastic rock, consisting of glass sand, was recovered in a dredge that may well be part of this or a similar outcrop.

4. SAMPLING AND ANALYTICAL METHODS

The dive samples were collected using ROV *Tiburon* during two cruises of the Monterey Bay Aquarium Research Institute's RV *Western Flyer* in March and May of 2000. The dredge samples were collected on multiple cruises of the U.S. Geological Survey [for details see *Davis et al.*, 2002].

The hyaloclastite samples were cut for standard and polished thin sections for microscope and electron microprobe analyses, respectively. The glasses were analyzed with a JEOL JX 8900 Superprobe at the U.S. Geological Survey in Menlo Park, using synthetic and natural glass and mineral standards. Details are described by *Davis et al.* [1994]. Volatile analyses were carried out with a Cameca IMS-6F ion probe at Carnegie Institute of Washington, Department of Terrestrial Magnetism, using methods described by *Hauri et al.* [2002].

5. DESCRIPTION OF HYALOCLASTITE

In accord with the broad definition for hyaloclastite [*Fisher and Schmincke,* 1984], all samples are predominantly composed of glass (>70%). The glass may be fresh, or partially to

Table 1. Location and Water Depth for Hyaloclastite Samples

Sample	Latitude (°N)	Longitude (°W)	Depth (m)	Sample type
Davidson Seamount				
T139-R4	35.772	122.691	1611	Monomict breccia
T140-R6	35.547	122.824	3077	Monomict hawaiite sandstone
T141-R8	35.634	122.770	2300	Polymict breccia
T142-R1	35.782	122.659	1871	Monomict breccia
T142-R5	35.785	122.665	1755	Polymict breccia
T142-R8	35.785	122.663	1748	Polymict breccia
T144-R6	35.564	122.786	2624	Monomict breccia
T145-R5	35.427	122.998	3380	Polymict basalt sandstone
T147-R1	35.720	122.724	1337	Polymict breccia
T147-R6	35.723	122.723	1281	Monomict breccia
T147-R8	35.724	122.722	1363	Polymict breccia
T147-R16	35.729	122.713	1580	Polymict volcanic conglomerate
L2-79D1-7	35.749	122.739	2060	Monomict volcanic conglomerate
L2-79D2-H3	35.752	122.680	1910	Bedded sandstone w.lapilli
L2-79D3-1	35.761	122.704	1840	Bedded sandstone
Guide Seamount				
T124-R4	36.974	123.367	1882	Monomict breccia
S4-78D2-15	37.022	123.330	2540	Polymict breccia

Note: Dredge and ROV dive tracks are shown in Figure 1. Locations for dredge samples have been averaged

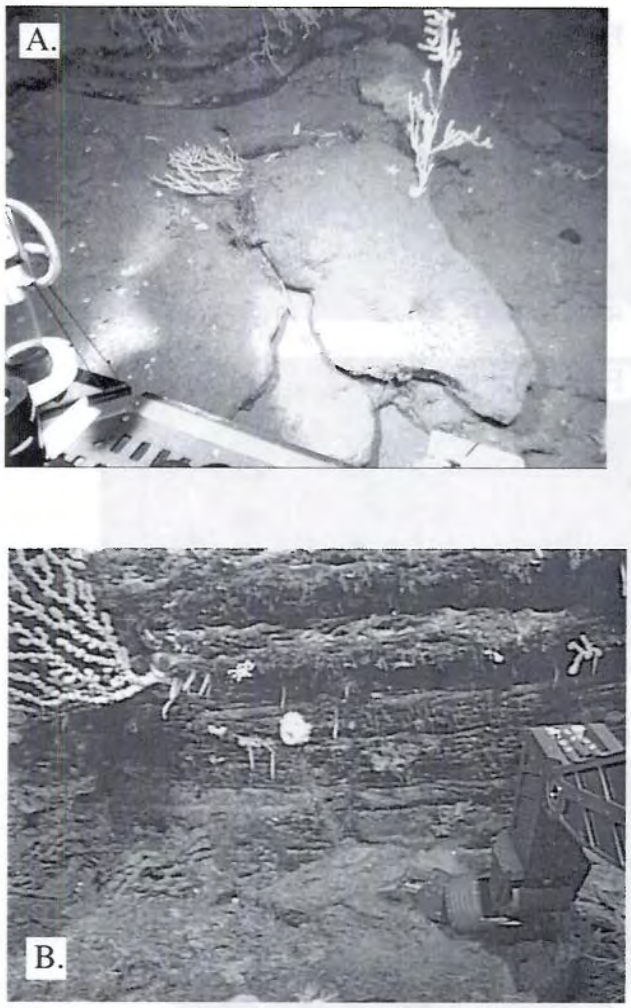

Figure 2. Photographs from ROV *Tiburon* video showing (A) slabby surface of typical hyaloclastite outcrop and (B) volcaniclastic sandstone outcrop. Field of view for both approximately 5 m.

completely altered to palagonite. We use the textural features in conjunction with the glass compositions to group the samples into six types that reflect their mode of origin. Based on glass chemistry (discussed in the next section), the samples are either mono- or polymict. Based on textural characteristics, we refer to them as breccia, volcanic conglomerate, and bedded or massive volcanic sandstone (Plate 1).

5.1. Monomict Breccia

The most common hyaloclastite samples recovered from each of the seamounts are monomict breccias composed of highly vesicular (to >50%), angular to subrounded glass fragments. The glass fragments (< 1mm to > several cm) are typically crystal rich, with microphenocrysts of euhedral olivine and plagioclase, plus complexly zoned clinopyroxene in some samples. Some of the bigger clasts may show a jigsaw puzzle fit (Plate 1a) indicating in situ brecciation of pillow wedges. In some samples the glass has been completely replaced by palagonite. Others have palagonite rims of variable thickness surrounding fresh glass cores. Virtually all samples contain at least traces of marine sediment and biologic debris (e.g. sponge spicules) in the interstices but some are largely clast-supported whereas others contain a larger proportion of clay matrix (Plate 1b). Minor tachylite is also present and appears to be related to the same flow, based on the phenocryst contents.

5.2 Polymict Breccia

Other, similar looking, hyaloclastite breccias are polymict with more than one glass composition (Table 2). All of these are matrix supported and some contain more diverse and more abundant rock fragments (Plate 1c), including small xenoliths and large xenocrysts of complexly zoned clinopyroxene and plagioclase with resorbed margins, and rare, rounded, and oxidized amphibole megacrysts. The most compositionally diverse glass grains are found in the polymict hyaloclastite (S5-78D2-15) from Guide Seamount (Plate 1c). This sample includes numerous tholeiitic glass spherules (Figure 3a) some of which are totally degassed with respect to sulfur (Table 2).

5.3 Volcanic Conglomerate

Two samples are poorly sorted conglomerates composed of lapilli-sized, sub-rounded to angular clasts that are extremely vesicular (>50%) and nearly crystal free glass (Plate 1d), compared to the breccias above. The glass is virtually unaltered, lacking the palagonite rim observed for many clasts in the breccias. No bedding is observed in these two samples but a third sample consists of a massive layer of lapilli-sized clasts that grades into bedded sand layers (Plate 1e).

5.4 Bedded Volcanic Sandstone

Two dredged samples are bedded volcanic glass sandstone. One has three to five repetitive layers grading from medium to fine sand and silt (Plate 1f). Based on the position of thick Mn crust on the samples, the grading is assumed to be normal. Most of the sand-sized grains are fresh glass but a large proportion of the silt is altered to palagonite and iron oxide. This unit may be from the unsampled, bedded outcrop observed on one of the dives (Figure 2b). The second sample consists of a sand layer

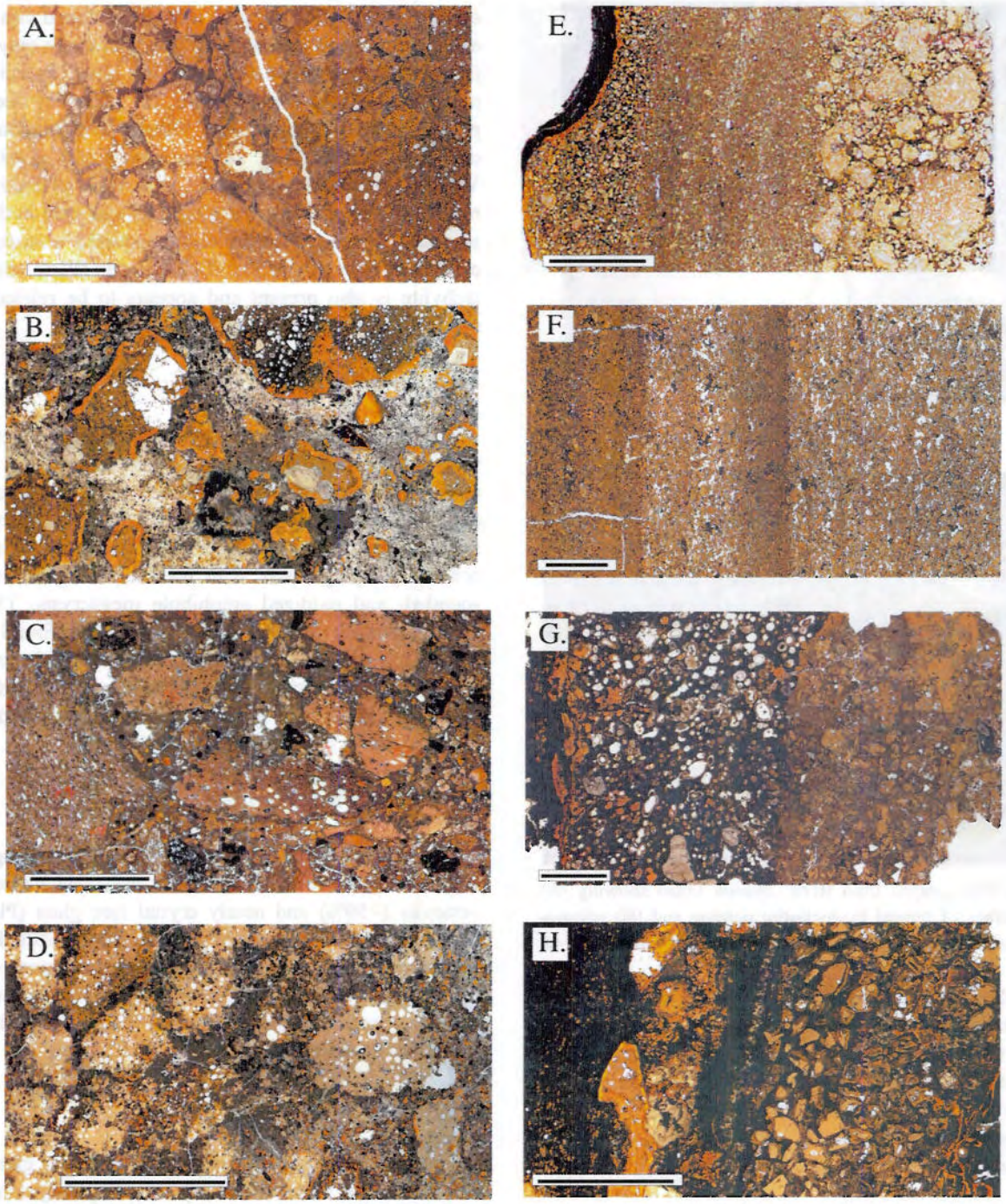

Plate 1. Photomicrographs of hyaloclastite thin sections. (A) monomict, clast-supported breccia (T124-R4), (B) monomict, matrix-supported breccia (T142-R5), (C) polymict breccia with a variety of glassy and lithic fragments (S4-78-D2-15), (D) volcanic conglomerate with highly vesicular, crystal-free pyroclasts (L2-79-D3-1), (E) layer of poorly-sorted lapilli-sized clasts in depositional contact with sand layers (L2-79-D2-H3), (F) bedded sandstone with multiple layers of angular glass shards (L2-79-D3-1), (G) monomict hawaiite sandstone (T140-R6) in contact with highly vesicular lava flow, (H) polymict basalt sandstone (T145-R5), with vesicle-free, angular glass in two layers separated by a band of manganese oxide. Top of section is to the left. Scale bar is 0.5 cm.

Table 2. Representative Glass Compositions

Sample	SiO_2	TiO_2	Al_2O_3	FeO	MnO	MgO	CaO	Na_2O	K_2O	P_2O_5	SO_3	Cl	Total
T139-R4 1	49.46	2.94	18.11	8.47	0.16	4.36	9.01	3.34	2.81	0.87	0.07	0.09	99.65
T139-R4 2	49.53	2.82	18.43	8.40	0.15	4.53	9.16	3.31	2.92	0.88	0.09	0.09	100.29
T140-R6 1	49.16	3.01	18.11	9.40	0.16	4.22	8.79	3.50	2.46	0.84	0.15	0.09	99.87
T140-R6 2	49.45	3.00	18.09	9.55	0.15	4.21	8.73	3.56	2.44	0.80	0.16	0.09	100.20
T140-R6 3	49.36	3.02	18.11	9.49	0.16	4.17	8.81	3.63	2.37	0.76	0.17	0.07	100.13
T141-R8 1	48.78	3.12	19.32	8.87	0.20	3.95	9.13	2.18	2.40	1.15	0.29	0.16	99.52
T141-R8 2	47.76	3.16	19.09	9.05	0.17	3.88	8.95	4.51	3.00	1.02	0.08	0.12	100.75
T141-R8 3	47.54	3.21	19.11	8.85	0.13	4.00	9.09	4.19	2.87	0.94	0.14	0.10	100.16
T141-R8 4	47.90	3.08	19.05	8.83	0.19	3.89	8.93	4.15	2.93	0.99	0.17	0.11	100.18
T142-R5 1	48.65	3.23	18.24	9.61	0.14	3.92	8.91	3.71	2.96	1.03	0.12	0.14	100.62
T142-R5 2	47.74	3.23	18.78	9.29	0.20	3.56	9.27	3.80	2.91	0.90	0.14	0.13	99.91
T142-R5 3	48.01	3.47	18.42	9.53	0.17	3.65	9.13	3.61	3.06	0.95	0.11	0.13	100.22
T144-R6 1	47.64	3.38	17.05	10.02	0.17	4.80	10.08	3.80	2.05	0.74	0.13	0.06	99.91
T144-R6 2	47.57	3.53	16.81	10.03	0.16	4.69	10.05	3.59	1.99	0.72	0.13	0.06	99.32
T144-R6 3	47.51	3.47	16.58	10.31	0.14	4.69	10.04	3.61	2.03	0.75	0.12	0.06	99.30
T144-R6 4	47.28	3.52	16.84	9.97	0.18	4.75	10.02	3.52	2.02	0.77	0.08	0.06	98.98
T145-R5 1	50.05	2.06	16.51	10.24	0.15	6.58	9.61	3.35	0.89	0.35	0.16	0.03	99.97
T145-R5 2	49.60	2.11	16.19	10.64	0.15	6.62	9.56	3.37	0.74	0.28	0.16	0.03	99.44
T145-R5 3	49.84	2.09	16.53	10.25	0.11	6.55	9.67	3.40	0.90	0.33	0.12	0.03	99.81
T145-R5 4	49.24	2.48	16.92	9.56	0.14	5.14	9.74	3.59	1.42	0.44	0.14	0.04	98.85
T145-R5 5	49.87	2.44	17.35	9.56	0.14	5.26	9.98	3.57	1.46	0.48	0.14	0.05	100.27
T147-R1 1	49.36	3.12	18.48	8.62	0.14	4.69	8.97	3.63	2.68	1.00	0.06	0.09	100.82
T147-R1 2	48.77	3.17	18.39	8.61	0.13	4.72	8.51	3.64	2.83	0.97	0.07	0.08	99.85
T147-R1 3	49.11	3.21	18.52	8.54	0.17	4.69	8.85	3.73	2.69	1.03	0.02	0.08	100.61
T147-R6 1	49.26	2.94	18.54	8.25	0.15	4.39	7.88	3.93	3.00	1.20	0.06	0.11	99.68
T147-R6 2	49.25	3.06	18.22	8.19	0.14	4.41	7.98	3.86	2.96	1.22	0.07	0.11	99.43
T147-R6 3	49.42	3.09	18.61	8.09	0.12	4.53	7.99	3.88	2.98	1.30	0.08	0.11	100.16
T147-R6 4	49.41	2.95	18.38	8.30	0.14	4.40	8.00	3.61	2.99	1.24	0.06	0.10	99.55
T147-R8 1	48.77	3.73	17.85	8.77	0.17	3.05	7.62	2.99	3.18	1.57	0.09	0.12	97.86
T147-R8 2	49.60	3.48	17.79	8.42	0.15	3.02	7.30	4.89	3.67	1.28	0.09	0.14	99.78
T147-R8 3	48.94	3.69	17.73	8.60	0.14	3.08	7.38	4.94	3.56	1.40	0.09	0.14	99.65
T147-R16 1	50.53	2.69	19.53	7.70	0.15	4.30	7.43	4.04	2.92	1.03	0.02	0.10	100.40
T147-R16 2	50.44	2.72	19.14	7.59	0.15	4.15	7.40	4.00	2.88	1.02	0.07	0.09	99.62
T147-R16 3	50.24	2.82	19.28	7.86	0.13	4.21	7.36	4.10	2.92	1.05	0.06	0.09	100.09
T147-R16 4	50.37	2.79	19.33	7.89	0.17	4.23	7.35	4.13	2.94	1.04	0.05	0.09	100.36
L2-79D1-7	48.24	3.75	16.83	10.05	0.17	4.70	10.21	2.83	2.20	0.66	0.05	0.06	99.83
L2-79D1-7	49.98	2.49	18.35	7.77	0.13	4.62	8.48	4.12	2.40	0.83	0.03	0.08	99.30
L2-79D1-7	50.39	2.53	18.35	7.70	0.11	4.72	8.58	4.11	2.49	0.86	0.02	0.09	99.98
L2-79D1-7	49.23	2.68	18.28	7.75	0.12	4.66	8.66	4.28	2.68	1.04	0.02	0.09	99.64
L2-79D2-H3	47.44	3.50	16.53	10.34	0.17	4.62	9.84	3.93	2.29	0.70	0.07	0.06	99.48
L2-79D2-H3	48.08	3.39	16.70	10.0	1.14	4.80	10.09	3.95	2.20	0.69	0.08	0.06	100.18
L2-79-D3-1	47.70	3.48	16.82	10.04	0.19	4.66	9.77	3.85	2.14	0.61	0.06	0.10	99.41
L2-79-D3-1	47.53	3.03	16.71	9.74	0.14	4.74	10.24	3.92	2.13	0.59	0.06	0.10	99.22
L2-79-D3-1	47.45	3.59	16.37	9.88	0.15	4.66	10.12	4.23	2.14	0.63	0.06	0.09	99.36
T124-R4 1	48.08	3.21	18.16	8.34	0.17	4.50	8.63	3.77	2.50	1.11	0.07	0.10	98.63
T124-R4 2	48.09	3.23	18.04	8.65	0.15	4.54	8.67	3.97	2.53	1.15	0.09	0.10	99.16
S4D2-15 1	52.09	2.52	16.88	8.82	0.16	4.79	7.92	3.70	1.63	0.57	0.04	0.06	99.16
S4D2-15 2	49.86	2.60	18.04	8.46	0.14	4.61	7.95	4.07	2.11	0.80	0.07	0.07	98.75
S4D2-15 3	51.74	2.81	17.71	8.21	0.19	3.15	5.68	4.38	3.35	0.95	0.02	0.13	98.29
S4D2-15 4	49.86	2.60	18.04	8.46	0.14	4.61	7.95	4.07	2.11	0.80	0.07	0.07	98.75
S4D2-15 5	51.28	2.97	17.02	8.96	0.17	3.73	7.14	4.03	2.80	1.10	0.02	0.10	99.29
S4D2-15 6	50.71	2.34	13.95	12.70	0.23	6.43	9.83	2.59	0.26	0.11	0.01	0.01	99.15
S4D2-15 7	50.60	2.37	13.95	13.27	0.26	6.24	9.94	2.69	0.33	0.22	0.00	0.00	99.87
S4D2-15 8	51.19	2.37	14.12	13.36	0.24	6.27	9.87	2.46	0.45	0.28	0.00	0.01	100.61
S4D2-15 9	50.05	2.44	13.72	13.12	0.23	6.41	10.15	2.61	0.24	0.19	0.00	0.01	99.17

overlying a poorly sorted layer of lapilli-sized clasts (Plate 1e) that was already described. The finer grained layers of this sample contain many small shards that are broken across vesicles, and rare curved fragments that may be bubble-wall fragments (Figure 3b).

5.5 Massive Hawaiite Sandstone

One hyaloclastite sample (T140-R6) is a massive, coarse sandstone of highly angular, vesicular glass shards. The glass is monomict hawaiite, similar in composition to that in the breccias but it is less vesicular and not as crystal rich (Plate 1g). Many glass grains have fluidal shapes, some with parallel, elongated vesicles (Figure 3c). Many of the non-vesicular fragments appear to be broken along vesicle margins (Figure 3c), indicating vesiculation before fragmentation. This fragmental layer is in contact with a highly vesicular, tachylitic lava flow that has the same crystal assemblage as the fragmental material, suggesting it is ejecta from the same eruption.

5.6 Massive Basalt Sandstone

One hyaloclastite sample (T145-R5), collected on the deepest dive (~3400 m), consist mostly of small (mm-size), angular, basalt glass shards. It is vesicle free and almost devoid of crystals (Plate 1h). It has two different glass compositions of transitional and mildly alkalic basalt in two distinct layers that are separated by a mm-thick band of manganese oxide.

6. GLASS COMPOSITIONS

Hawaiite is the most common composition of hyaloclastite glass. Both alkalic basalt and mugearite are present but much less abundant than in the associated lavas [*Davis et al.,* 2002]. Except for two samples, the glass compositions of hyaloclastites from Davidson Seamount (Table 2) closely match those of quenched rinds of lava samples collected nearby. The basalt glass in the sample from the deepest dive (T145-R5) on Davidson Seamount has no comparable flow composition. The most evolved glass composition in the polymict breccia of T147-R8 also has no corresponding lava sample but similar mugearite whole rock compositions were found at other locations on Davidson, as well as on Guide and Rodriguez seamounts [*Davis et al.,* 1995; *Davis et al., 2002*].

Except for TiO_2, glass compositions of monomict samples are within analytical precision for major elements (Table 2). Variations in TiO_2 reflect different amounts of

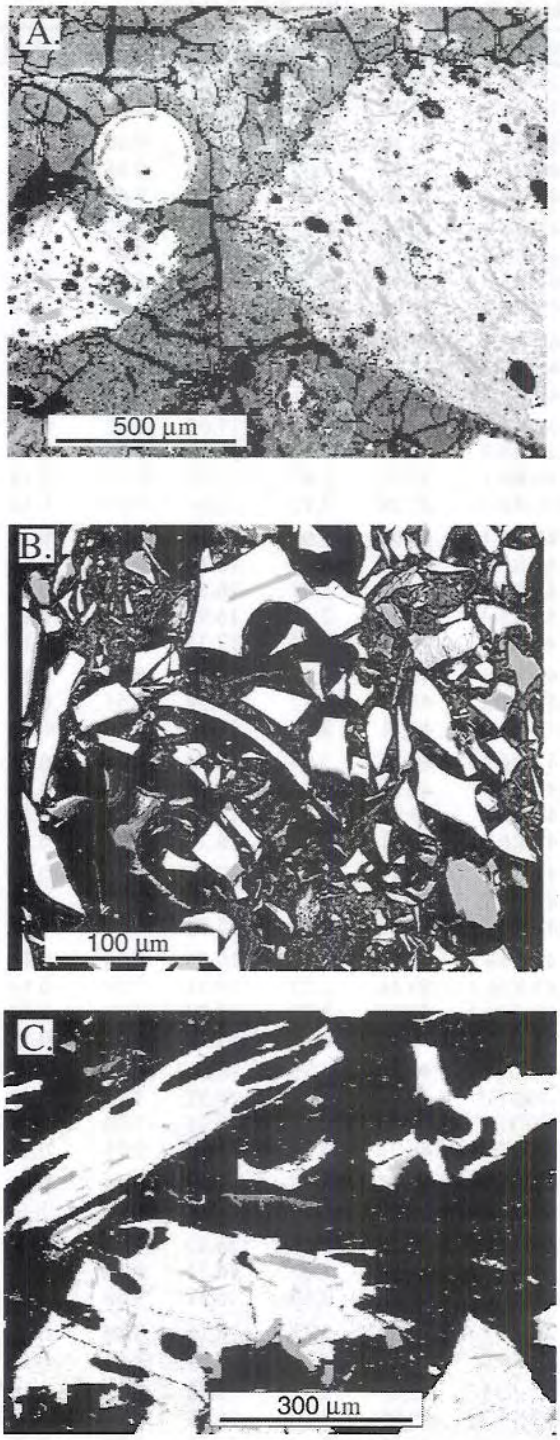

Figure 3. Back scattered electron images of (A) degassed, tholeiitic spherules and crystal-rich pyroclasts in polymict breccia from Guide Seamount, (B) Curved, broken glass shards in fine grained layer of bedded sandstone, (C) fluidal and curved glass fragments in monomict hawaiite sandstone from Davidson Seamount.

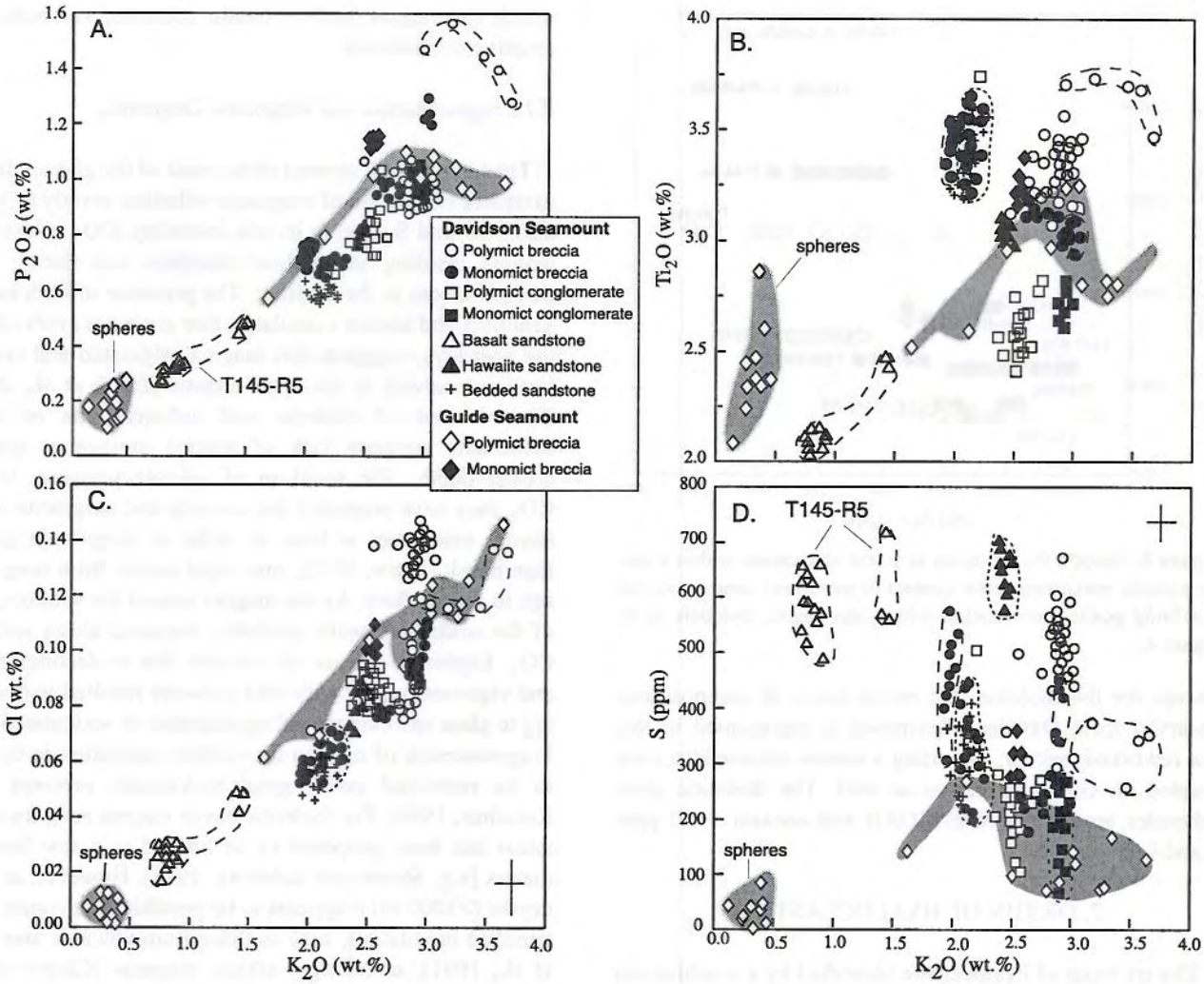

Figure 4. Composition of glass fragments in hyaloclastite samples. (A) K_2O vs. P_2O_5 shows a narrow range for monomict samples. (B) TiO_2 vs. K_2O shows a considerable range of TiO_2 at a given K_2O, reflecting titanomagnetite crystallization. (C) Cl vs. K_2O shows a positive correlation, indicating that Cl behaved as an incompatible element and did not degas significantly. (D) S vs. K_2O shows a large range at a given K_2O, indicating extensive degassing during an eruption. Gray field encloses compositions found in polymict breccia (S5-78D2-15) from Guide Seamount. Dashed lines indicate range of compositions in some other samples.

titanomagnetite fractionation. Because K_2O and P_2O_5 behaved as incompatible elements and are well correlated (Figure 4a), we use these elements as the main indicator to identify mono-or polymict samples. The glasses are generally high in Cl (300 - 1500 ppm). Cl is positively correlated with K_2O (Figure 4c), indicating that it behaved as an incompatible element. S, in contrast, shows a large range in abundance (<100-700 ppm) at a similar K_2O (Figure 4d). S varies by more than 200 ppm (Figures 4d, 5) for grains within single samples that have other elements within analytical precision. The highest values are observed for the non-vesicular basalt glass in the sample collected at ~3400 m water depth. Despite a considerable range in S abundance, there is a positive correlation between the maximum S content of monomict glass samples and collection depth (Figure 5).

The glass from the monomict breccia from Guide Seamount (T124-R4) is compositionally similar to hawaiite from Davidson Seamount. However, the polymict breccia (S5-78D2-15) contains glass fragments of highly diverse compositions, including hawaiite, mugearite, mildly to moderately alkalic basalt, and tholeiitic basalt (Figure 4).

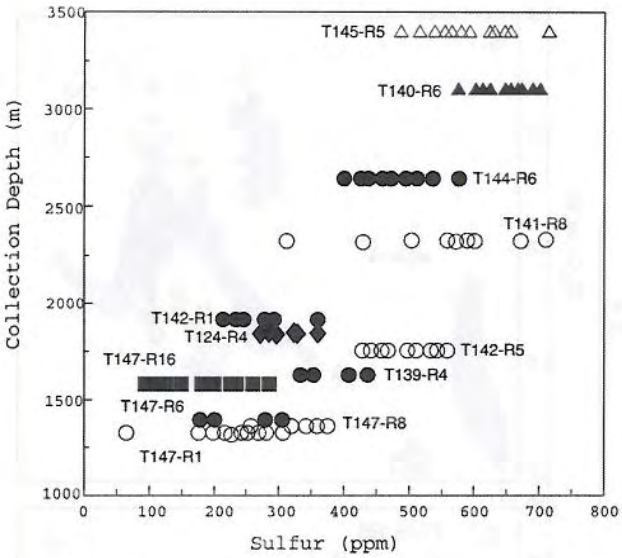

Figure 5. Despite the variation in sulfur abundance within a single sample, maximum sulfur content of monomict samples shows a definite positive correlation with water depth. Symbols as in Figure 4.

Except for the tholeiite, the entire range of compositions observed from Davidson Seamount is represented in this one reworked breccia, indicating a similar diverse lava suite erupted on Guide Seamount as well. The tholeiitic glass spherules are similar to E-MORB and contain <100 ppm S and Cl.

7. ORIGIN OF HYALOCLASTITE

The six types of hyaloclastite identified by a combination of chemistry, grain size, and textural features reflect differences in fragmentation and eruptive style, location relative to the vents, and post-eruptive sedimentary reworking. The types of eruptive products, whether subaerially or subaqueously erupted, are largely controlled by magma composition which determines initial volatile contents, viscosity, and eruptive temperature.

7.1 Fragmentation and Magmatic Degassing

The high vesicle content of the most of the glass indicates extensive exsolution of magmatic volatiles, mainly CO_2, but also H_2O and S. Due to its low solubility, CO_2 is lost from magma residing in shallow chambers and during slow magma ascent to the seafloor. The presence of both mantle xenoliths and alkalic cumulates, that are more evolved than the host lava, suggests that magma originated and crystallized extensively in the upper mantle [*Davis et al.*, 2002]. The absence of calderas and collapse pits on these seamounts suggests lack of magma storage at shallow crustal depth. The build-up of volatile pressure, largely CO_2, may have propelled the hawaiite and mugearite melts, having viscosities at least an order of magnitude greater than basalt [Shaw, 1972], into rapid ascent from deep storage to the seafloor. As the magma neared the seafloor, part of the sulfur and water probably degassed along with the CO_2. Explosive release of volatiles due to decompression and vigorous impact with cold seawater resulted in quenching to glass and extensive fragmentation of vesiculated lava. Fragmentation of magma by volatile exsolution is thought to be restricted under great hydrostatic pressure [e.g. *Kokelaar*, 1986]. For tholeiitic basalt magma such fragmentation has been proposed to be limited to a few hundred meters [e.g. *Moore and Schilling*, 1973]. However, at great depths (>3000 m) it appears to be possible for magma more enriched in volatiles, such as those from volcanic arcs [Gill et al., 1991], or strongly alkalic magmas [*Clague et al.*, 2002], including strongly evolved alkalic compositions such as those described here.

The majority of glass compositions from the seamounts had high initial volatile contents. CO_2 is highly incompatible during melting of the mantle and is positively correlated

Table 3. Ion Probe Analyses of Volatiles

Sample	T124-R4	T139-R6	T144-R12	T146-R24
Rock type	Hawaiite	Hawaiite	Alk.basalt	Mugearite
H_2O wt%	0.61	0.69	0.63	0.67
CO_2 ppm	31	51	79	69
F ppm	1791	1139	1179	1582
S ppm	427	446	686	598
Cl ppm	1387	1242	716	1231

Note: only T124-R4 is hyaloclastite, but analysis is not of same grain as for microprobe. Other samples are pillow rims. Analyses are average of 4 to 5 separate analyses.

with Nb [*Hauri et al.*, 2002; *Saal et al.*, 2002]. Based on a constant CO_2/Nb ratio in MORB [~ 273 to 317, *Hauri et al.*, 2002; *Saal et al.*, 2002] these magmas could have had maximum CO_2 contents ranging from 1.7 wt.% for alkalic basalt to >4.2 wt.% for mugearite. The Ce/H_2O ratio is also constant in MORB [174 -223, *Hauri et al.*, 2002] and H_2O contents calculated from Ce concentrations of whole rock samples [*Davis et al.*, 2002] range from 1.1% to >4.2% for alkalic basalt and mugearite, respectively. The estimates for mugearite are minima since Nb and Ce are no longer incompatible elements due to crystallization of Fe-Ti oxides and apatite. Application of these MORB ratios seems reasonable since the isotopic compositions of samples from these seamounts suggest small degrees of partial melting of MORB-like mantle sources [*Davis et al.*, 2002]. Ion probe analyses of several seamount glasses have H_2O ranging from 0.5 to 0.7% and CO_2 <100 ppm (Table 3), clearly indicating extensive exsolution and loss of these volatiles. *Dixon* [1997] and *Dixon et al.* [1997], using measured solubilities of CO_2 and H_2O in alkaline melts, have modeled the exsolution of magmatic gases from alkalic magmas and shown that significant amounts of H_2O (and S) are exsolved along with CO_2 as bubbles form. Exsolution of the estimated initial volatiles in these magmas would lead to vesicle contents even higher than those observed, suggesting that some portion of the gas has escaped from the rising magma.

Cl and F are positively correlated with K_2O and apparently did not degas significantly. S, however, undoubtedly degassed to some extent, probably both during formation of vesicles when magma reached shallow depth and during eruption on the seafloor. The decrease in S at a given K_2O (Figure 4d) by about 200 ppm for clasts within nearly every monomict sample, regardless of water depth (Figure 5), reflects at least that much degassing of S occurs during eruption.

7.2. Eruption Style

Comparably gas-rich lava erupted subaerially would have produced significant Hawaiian-style lava fountains [e.g. *Head and Wilson*, 2002]. The monomict breccias and volcanic conglomerates have highly vesicular (>50%), angular to rounded clasts. They resemble scoria of cinder cones, except they are all glassy indicating quenching in water. The fluidal and curved glass shapes (Figures 3b,c) found in the finer-size fraction of multiple samples appear to be analogous to aerodynamic shapes found in subaerial fire fountains [*Vergionelle and Mangan*, 2000]. Since no one has observed explosive eruptions in the deep sea, comparison with subaerially erupted ejecta provides the only clues to eruption styles. Although much of the fragmentation may have resulted from shattering of already vesiculated lava, we interpret theses textural features as evidence for Hawaiian-style fountains, probably of low height depending on eruption depth. Pele's hair, characteristic of Hawaiian fountains, was not observed, although its absence may simply indicate that such delicate fragments are unrecognizable after more than 10 m.y. of alteration. Large, irregular, gas cavities in some lava samples indicate that the exsolved gases may have coalesced and escaped in bursts through the vent. In this case, Strombolian activity may have occurred as well. Expansion of steam due to entrapment of water or wet sediment is probably a common occurrence in subaqueous eruptions. Formation of bubble-wall fragments attributed to steam expansion has been described from deep sea eruptions at near-ridge seamounts [e.g. *Maicher and White*, 2002] and from Loihi seamount [*Clague et al.*, 2000]. The presence of such glass shapes at spreading centers [*Clague et al.*, this volume] and from water depths (>3000 m) that would restrict steam expansion, suggests discharge of a separated gas phase, probably CO_2, may be the driving mechanism. Rare, curved glass fragments, found in some samples (Figure 3b), could be pieces of bubble walls that were broken during transport. However, pyroclast shapes such as spindle bombs or agglutinated spatter that are indicative of Strombolian eruptions were not observed. Rapid quenching in water would probably prevent welding and agglutinating of particles.

Although the mixing of hot rock or magma with water must have led to production of steam, we have found no evidence for large scale phreatic, or phreatomagmatic eruptions on any of the seamounts. Such evidence would consist of lithic fragments of country rock in the hyaloclastite deposits. Extensive phreatic eruptions of basaltic composition commonly accompany caldera or pit crater collapse [e.g., *McPhie et al.*, 1990; *Clague et al.*, this volume], which expose large amounts of hot rock or magma to water. Bathymetric surveys of each of these seamounts show that such collapse structures are notably absent [*Davis et al.*, 2002]. Diverse chemistry of flows and the small volume of individual cones on the seamounts also suggest eruption of small magma volumes thereby providing a limited heat source.

Since episodes of volcanic activity apparently were separated by long time intervals [*Davis et al.*, 2002], the initial eruptions must have had enough gas pressure to open conduits to the surface. Hence the earliest stage of eruption may have started with small-scale, vulcanian-like ejection of country rock clearing the vent. Although some lithic fragments, xenoliths, and broken crystals were observed, especially in the

polymict breccias, no unit resembling typical vulcanian deposits was observed. However, the material ejected in an earlier, explosive phase would probably be covered by later lavas and by the fallout from the eruption column.

Despite similar hawaiite composition, the volcanic conglomerates contain generally more vesicular pyroclasts than the breccias but they are virtually free of crystals. Based on the S content, these samples erupted in water depths comparable to or slightly deeper than the crystal-rich breccia samples. Since a high crystal content increases viscosity and inhibits bubble expansion [*Cashman et al.* 2000], these magmas may have had slightly lower viscosity due to more rapid ascent and/or higher effusion rates. Although fragmentation caused by gas exsolution is indicated for the breccias, the jigsaw puzzle fit of some larger clasts suggests that in-situ cooling contraction granulation [*Kokelaar*, 1986] further fragmented some clasts (Plate 1a). The monomict hawaiite sandstone with angular, moderately vesicular clasts erupted in deeper water (3077 m), resulting in lower vesicle and higher S content (Figure 4d). Despite the greater eruption depth, many glass fragments have fluidal shapes and are broken across vesicles, suggesting fragmentation from gas exsolution; they probably formed in Hawaiian-style fountains of limited height. In contrast, the basaltic sandstone from the deepest site (~3400 m) consists of crystal- and vesicle-free, angular glass shards (Plate 1h) that probably resulted mostly from cooling contraction granulation processes. Textures of this sample are similar to hyaloclastite from near-ridge seamounts [e.g. *Smith and Batiza,* 1984; *Davis and Clague*, 2000] that appear to consist mostly of quench granulation fragments and spalled off pillow rinds. Due to a combination of lower initial volatile content of this transitional to mildly alkalic basalt and deeper eruption depth, fragmentation was not explosive. These deposits do not appear to be extensive.

7.3. Eruption Depths and Post-Eruptive Subsidence

S is sensitive to temperature, oxygen and sulfur fugacity, FeO content of the lava, and hydrostatic pressure. The positive correlation of maximum S content with increasing water depths (Figure 5) for comparable hawaiite and mugearite compositions can be attributed to changes in hydrostatic pressure, due to eruption at different water depths. On Davidson Seamount, hyaloclastite samples were collected in water depths ranging from 1300 to 3400 m. Many of these samples apparently erupted in shallow water, as seen by their low dissolved volatile contents and oxidized olivine in some flow samples. Partially rounded pyroclasts with concentric rims of palagonite, including some with reddish brown color, suggest ejection in shallow water; some tephra may have been projected subaerially. Although we are unable with the data at hand to reliably estimate this subsidence, we suspect up to 1000 m of subsidence may have occurred at these seamounts. Evidence for emergence, in the form of wave-cut erosion on Rodriguez Seamount offshore southern California, suggests subsidence of about 700 m since it's formation. Such magnitude of subsidence appears reasonable, based on subsidence documented for sedimentary sequences associated with volcanic rocks from the continental margin [*Wilson et al.*, 2002]. With this interpretation, eruption depths for the hyaloclastite on Davidson Seamount may have ranged from less than a few hundred m to over 2000 m.

The low S contents of tholeiitic glass spherules found in the polymict breccia from Guide Seamount is indicative of subaerial eruption but would imply subsidence of ~1700 m for Guide Seamount. No source vent for these spherules has been identified. The eruption of tholeiitic basalt following the eruption of fractionated alkalic lavas contrasts with the evolution typically observed on ocean islands. It is possible that these spherules were transported here from Miocene, tholeiitic, basaltic volcanoes in the Coast Range of southern California [*Cole and Basu*, 1995].

7.4. Deposition and Post-Eruptive Reworking

The coarseness of the ejecta and the massive, poorly sorted, clast-supported texture of the breccia and conglomerate samples suggest limited dispersal. Most likely these particles are fallout from an eruption column of limited height and were deposited near vent sites, forming the discontinuous slabs observed on the dives. Similar monomict breccia samples that have a larger proportion of finer sediment in the matrix probably were transported somewhat farther from their eruption site.

The polymict, matrix-supported breccias probably are reworked deposits and include a range of glass compositions and a larger variety of lithic clasts as well as abundant biogenic debris, which were entrained when currents displaced them into deeper water. They do not represent single eruptive events. While these polymict hyaloclastites provide less information concerning eruptive processes related to a single event, they are useful in giving an indication of the range of processes and overall compositional range of ejecta present on the seamount. The diverse glass compositions in the polymict breccia (S5-78D2-15) from Guide Seamount clearly demonstrate the great range of compositions erupted, including mildly to moderately alkalic basalt, hawaiite, and mugearite.

The bedded volcanic sandstones have a narrow range of glass compositions spanning multiple layers. The composite sample of lapilli-sized clasts and sand also consists of a common glass composition. They apparently each formed during a single eruptive event. In some respect, they resemble base surge deposits of phreatomagmatic eruptions but apparently were less energetic. No dunes, antidunes, ripples or cross-bedding, common in such deposits [*Fisher and Schmincke*, 1984], were observed. Most likely these samples formed from a slurry of tephra and water, deposited by density currents directly related to volcanic activity [*White*, 2000; *Smellie*, 2001].

8. CONCLUSIONS

Hyaloclastite deposits on mid-Miocene seamounts offshore central California have predominantly evolved alkalic basalt glass compositions. Fragmentation occurred primarily due to exsolution of magmatic gases and interaction of hot magma with cold seawater. Textures suggest formation during mildly explosive eruptions with Hawaiian-style fountains of limited height. Monomict samples with coarse-grained pyroclasts and little or no sediment matrix settled near the vents, whereas polymict, matrix-supported samples were reworked and deposited in deeper water, farther from vent sites. Based on glass composition, the multiple layers of the bedded sandstone formed during a single eruptive event. Less volatile-rich, mildly alkalic basaltic glass in the hyaloclastite from the deepest site apparently formed by quench granulation processes. Eruption depths ranged from near sea level to over 2000 m, suggesting a large amount of subsidence for these seamounts.

Acknowledgments. Support by the David and Lucile Packard Foundation is gratefully acknowledged. J. Paduan helped prepare Figure 1. Helpful reviews by R. Batiza, J. Smellie, and especially D. Maicher improved the manuscript.

REFERENCES

Batiza, R., D.J. Fornari, D.A. Vanko, and P. Lonsdale, Craters, calderas and hyaloclastites on young Pacific seamounts, *J. Geophys. Res.*, *89*, 8371-8390, 1984.

Batiza, R., and J. D.L. White, Submarine lavas and hyaloclastite, in *Encyclopedia of Volcanoes*, edited by H. Sigurdsson (et al.), Academic Press, San Diego, 361-381, 2000.

Clague, D.A., A.S. Davis, J.L. Bischoff, J.E. Dixon, and R. Geyer, Lava bubble-wall fragments formed by submarine hydrovolcanic explosions on Loihi Seamount and Kilauea Volcano, *Bull. Volcanol.*, *61*, 437-449, 2000.

Cashman, K.V., B. Sturtevat, P. Papale, and O. Navon, Magmatic fragmentation, in *Encyclopedia of Volcanoes*, edited by H. Sigurdsson, (et al.), Academic Press, San Diego, 421-430, 2000.

Clague, D.A., R.T. Holcomb, J.M. Sinton, R.S. Detrick, and M.E. Torresan, Pliocene and Pleistocene alkalic flood basalts on the seafloor north of the Hawaiian Islands, *Earth. Planet. Sci. Lett.*, *98*, 299-349, 1995.

Clague, D.A., K. Uto, K. Satake, and A.S. Davis, Eruption style and flow emplacement in the submarine North Arch volcanic field, Hawaii, in *Hawaiian Volcanoes: Deep Underwater Perspectives*, edited by E. Takahashi (et al.), Am. Geophys. Union Monograph 128, Washington D.C., 65-84, 2002.

Cole, R.B., and A.R. Basu, Nd-Sr isotopic geochemistry and tectonics of ridge subduction and middle Cenozoic volcanism in western California, *Geol. Soc. Am. Bull.*, *107*, 167-179, 1995.

Davis, A.S., and D.A. Clague, President Jackson Seamounts, northern Gorda Ridge: tectonomagmatic relationship between on- and off-axis volcanism, *J.Geophys. Res.*, *105*, 27939-27956, 2000.

Davis, A.S., D.A. Clague, W.A. Bohrson, G.B. Dalrymple, and H.G. Greene, Seamounts at the continental margin of California: A different kind of oceanic volcanism, *Geol. Soc. Am. Bull.*, *114*, 316-333, 2002.

Davis, A.S., D.A. Clague, and W.B. Friesen, Petrology and mineral chemistry of basalt from the Escanaba Trough, southern Gorda Ridge, *U.S. Geol Surv. Bull.*, *2022*, 153-170, 1994.

Davis, A.S., S.H. Gunn, W.A. Bohrson., L.B. Gray, and J.R. Hein, Chemically diverse sporadic volcanism at seamounts offshore southern and Baja California, *Geol. Soc. Am. Bull. 107*, 554-570, 1995.

Dixon, J.E., Degassing of alkalic basalts, *Am. Mineralogist, 82*, 368-378, 1997.

Dixon, J.E., D.A. Clague, P. Wallace, and R. Poreda, Volatiles in alkalic basalts from the North Arch volcanic field, Hawaii: Extensive degassing of deep submarine-erupted alkalic series lavas, *J. Petrol.*, *38*, 911-939, 1997.

Fisher, R.V., and H.-U. Schmincke, *Pyroclastic rocks*, Springer-Verlag, Berlin, 472 p., 1984.

Gill, J., P. Torssander, H. LaPierre, R. Taylor, K. Kaiho, M. Koyama, M. Kusakabe, J. Aitchison, S. Cisowski, K. Dadey, K. Fujioka, A. Klaus, M. Lovell, K. Marsaglia, P. Pezard, B. Taylor, and K. Tazaki, Explosive deep water basalt in the Sumisu backarc rift, *Science, 248*, 1214-1217, 1990.

Hauri, E., K. Gronvold, N. Oskarsson, and D. McKenzie, Abundance of carbon in the Icelandic mantle: constraints from melt inclusions, *Trans. Am. Geophys. Union, EOS.*, 2002.

Hauri, E.H., J. Wang, J.E. Dixon, P.L. King, C. Mandeville, S. Newman, SIMS analysis of volatiles in silicate glasses, 1: Calibration, matrix effects and comparisons with FTIR, *Chem. Geol.*, in press, 2002.

Head, J.W., III, and L. Wilson, Deep submarine pyroclastic eruptions: Theory and predicted landforms and deposits, *J. Volcano. Geotherm. Res.*, in press, 2002.

Kokelaar, B.P., Magma-water interactions in subaqueous and emergent basaltic volcanism, *Bull. Volcanol., 48*, 275-289, 1986.

Lonsdale, P., Structural patterns of the Pacific floor offshore of peninsular California. *In The gulf and peninsular province of the Californias*, edited by Dauphin (et al.), *Am. Ass. Petrol. Geol. Mem. 47*, 87-125, 1991.

Maicher, D., and J.L. White, The formation of deep-sea Limu o Pele, *Bull. Volcanol., 63*, 482-496, 2001.

McPhie, J., G.P.L. Walker, and R.L. Christiansen, Phreatomagmatic and phreatic fall and surge deposits from explosions at Kilauea Volcano, Hawaii, 1790 A.D.: Keanakakoi Ash Member, *Bull. Volcanol., 52*, 334-354, 1990.

Moore, J.G., and W.W. Chadwick, Jr., Offshore geology of Mauna Loa and adjacent areas, Hawaii, in *Mauna Loa Revealed: Structure, composition, history, and hazards*, edited by J.M. Rhodes and J.P. Lockwood, *Am. Geophys. Union Monograph 92*, 21-44, 1995.

Moore, J.G., and J.G. Schilling, Vesicles, water, and sulphur in Reykjanes ridge basalts, *Contrib. Mineral. Petrol., 41*, 105-118, 1973.

Saal, A.E., E.H. Hauri, C.H. Langmuir, and M.R. Perfit, Vapor undersaturation in primitive mid-ocean ridge basalt and the volatile content of the Earth's upper mantle, *Nature*, in press, 2002.

Shaw, H.G., Viscosities of magmatic silicate liquids: an empirical method of prediction, *Am. J. Sci., 272*, 870-893, 1972.

Smellie, J.L., Lithofacies architecture and construction of volcanoes erupted in englacial lakes: Icefall Nunatak, Mount Murphy, eastern Marie Byrd Land, Antarctica. *Spec. Publs int. Ass. Sediment, 30,* 9-34, 2001.

Smith, T., and R. Batiza, New field and laboratory evidence for the origin of hyaloclastite flows on seamount summits, *Bull. Volcanol., 51*, 96-114, 1989.

Staudigel, H., and H.-U. Schmincke, The Pliocene seamount series of La Palma (Canary Islands), *J. Geophys. Res., 89*, 11,195-11,215, 1984.

Vergniolle, S. and M. Mangan, Hawaiian and Strombolian eruptions in *Encyclopedia of Volcanoes*, edited by H. Sigurdsson (et al.), Academic Press, San Diego, 447-461, 2000.

White, J.D.L., Subaqueous eruption-fed density currents and their deposits, *Precamb. Res., 26,* 87-109, 2000.

Wilson, D. S., P.A. McCrory, and R.G. Stanley, Implications of volcanism in coastal California for the deformation history of western North America, *Tectonics*, in press, 2002.

Alicé S. Davis, David A. Clague, Monterey Bay Aquarium Research Institute, 7700 Sandholdt Road, Moss Landing, CA 95039-9644

Davis and Clague (2003).